would not pass through insert membranes, 12 control wells were prepared without postnatal tissue. At 20 to 23 DIV, cover slips were tested for trypan blue exclusion. No viable cells were found to have passed through insert membranes. Postnatal cells were patch-clamped at 20 to 27 DIV. Those generating APs were injected with 0.2% dextran fluorescein (Molecular Probes; –500 pA, 10 Hz, 30 min) for later identification. Then cells were fixed, treated with 2N HCl (37°C for 30 min), 0.1 M borate buffer (25°C for 10 min), and immunoreacted with sheep anti-BrdU (1:100; Fitzgerald), followed by rhodamine-conjugated secondary antibody (1:40; Jackson ImmunoResearch). Fluorescein-filled cells were identified with confocal microscopy and evaluated for BrdU-immunoreactivity by two independent observers.

31. Studies approved by the University of Minnesota Animal Care and Use Committee.

32. We thank A. Frankfurter for the gift of TuJ1, P. Letourneau and I. Fischer for critical evaluation of the manuscript, L. Furcht for generously supplying laminin, D. Snow and S. Kilo for constructive suggestions, K. Hargreaves for encouragement, and M. Wessendorf, L. Stone, and G. Sedgewick for microscopic and photographic assistance. Supported by a National Institute of Dental Research Dentist-Scientist Award (L.J.K, grant DE00225), National Institute on Drug Abuse (NIDA) training grant (C.A.F. grant DA07234, and T.M.L., grant DA07097), and NIDA R01 and Research Scientist Development Awards (G.L.W., grants DA01933 and DA04274).

10 October 1996; accepted 28 February 1997

Control of Inflammation, Cytokine Expression, and Germinal Center Formation by BCL-6

Alexander L. Dent, Arthur L. Shaffer, Xin Yu, David Allman, Louis M. Staudt*

The gene encoding the BCL-6 transcriptional repressor is frequently translocated and mutated in diffuse large cell lymphoma. Mice with a disrupted BCL-6 gene developed myocarditis and pulmonary vasculitis, had no germinal centers, and had increased expression of T helper cell type 2 cytokines. The BCL-6 DNA recognition motif resembled sites bound by the STAT (signal transducers and activators of transcription) transcription factors, which mediate cytokine signaling. BCL-6 could repress interleukin-4 (IL-4)–induced transcription when bound to a site recognized by the IL-4–responsive transcription factor Stat6. Thus, dysregulation of STAT-responsive genes may underlie the inflammatory disease in BCL-6–deficient mice and participate in lymphoid malignancies.

Diffuse large cell lymphoma is a common and aggressive subtype of B cell non-Hodgkin's lymphoma that frequently harbors genetic alterations in the BCL-6 gene: Up to 45% of these lymphomas contain BCL-6 translocations and 73% have mutations in a putative 5′ regulatory region of the gene (*1*). Because these genetic changes invariably spare the BCL-6 coding region, the contribution of BCL-6 to lymphomagenesis is likely to be a subversion of its role in nontransformed cells. Consistent with this possibility, BCL-6 protein is expressed at the highest levels in germinal center B lymphocytes, which are the cells from which diffuse large cell lymphomas may arise (*2–5*). BCL-6 is a potent transcriptional repressor, but its natural target genes have not been identified (*6–8*). To determine the normal biological function of BCL-6, we disrupted BCL-6 in the mouse germ line.

Using embryonic stem cell methodology (*9*), we deleted a portion of the BCL-6 locus encoding the zinc finger DNA binding domain of the protein (*10*) (Fig. 1A) and confirmed the structure of the mutant locus by Southern (DNA) blot analysis of tail DNA (Fig. 1B). No BCL-6 protein derived from the targeted locus could be detected in either heterozygous (+/−) or homozygous (−/−) BCL-6 mutant mice (*11*) (Fig. 1C).

BCL-6$^{+/-}$ mice appeared normal and BCL-6$^{-/-}$ mice were born with a normal Mendelian frequency and size. However, beginning a few days to 3 weeks after birth, BCL-6$^{-/-}$ mice displayed variable degrees of growth retardation and ill health. About half of the BCL-6$^{-/-}$ mice were sickly and died before 5 weeks of age. Roughly 20% of BCL-6$^{-/-}$ mice appeared grossly healthy and were similar to wild-type littermates with respect to flow cytometric analysis of bone marrow, splenic, and thymic lymphocyte populations (*12*).

Pathological examination of the BCL-6$^{-/-}$ mice revealed a prominent myocarditis and pulmonary vasculitis that probably contributed to the animals' illness and death. Myocarditis was observed in 82% of the BCL-6$^{-/-}$ mice examined, and 73% of the mice had evidence of pulmonary vasculitis (Fig. 2), but neither pathology was observed in wild-type littermates. The cellular infiltrates in the hearts and lungs were composed of mononuclear cells and polymorphonuclear cells, virtually all of which were eosinophils (Fig. 2). Although inflammatory disease was generally correlated with ill health

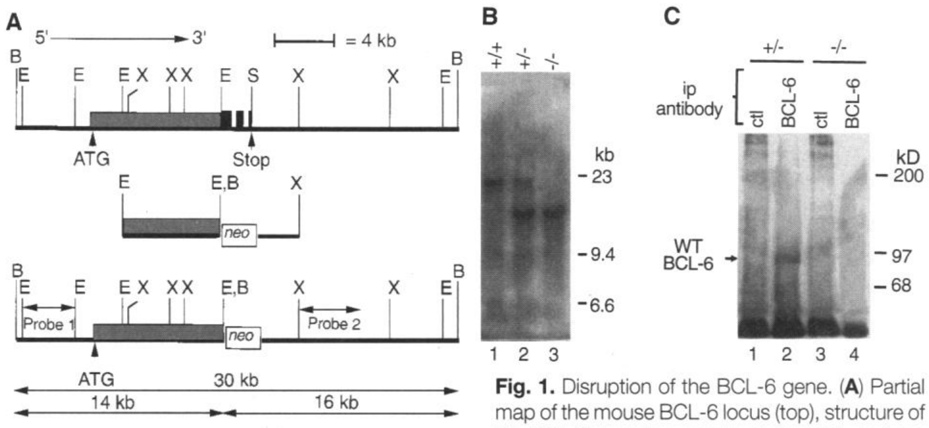

Fig. 1. Disruption of the BCL-6 gene. (**A**) Partial map of the mouse BCL-6 locus (top), structure of the BCL-6 targeting construct (middle), and the targeted BCL-6 allele (bottom). Mapped exons corresponding to the disrupted zinc finger domains are indicated by black boxes; the unmapped coding region is indicated by a grey box. The mutated BCL-6 locus would encode a truncated protein in which four of the six BCL-6 zinc fingers are disrupted and which cannot bind DNA in vitro (*16*). Restriction enzyme sites: B, Bam HI; E, Eco RI; S, Spe I; X, Xho I. *neo* = PGK-neomycin^r cassette. (**B**) Southern blot analysis of mice derived from intercrossing BCL-6$^{+/-}$ mice. Bam HI–digested tail DNA from wild-type mice (+/+) and mice heterozygous (+/−) or homozygous (−/−) for the disrupted BCL-6 allele was analyzed with a genomic flanking probe [probe 2 in (A)]. The structure of the targeted BCL-6 allele was also confirmed using probe 1 (A). (**C**) Analysis of wild-type and mutated BCL-6 protein expression. Spleen cells from immunized BCL-6$^{+/-}$ and BCL-6$^{-/-}$ mice were assayed for BCL-6 protein expression by immunoprecipitation followed by protein immunoblotting (*11*). Wild-type BCL-6 migrates at 90 to 100 kD (*2–5*) (lane 2); the truncated BCL-6 protein encoded by the targeted BCL-6 allele, predicted to be 12 kD smaller than the wild-type protein, was not detectable. ctl, control.

A. L. Dent, A. L. Shaffer, X. Yu, L. M. Staudt, Metabolism Branch, National Cancer Institute, National Institutes of Health, Bethesda, MD 20892, USA.
D. Allman, Experimental Immunology Branch, National Cancer Institute, National Institutes of Health, Bethesda, MD 20892, USA.

*To whom correspondence should be addressed. E-mail: lstaudt@alw.nih.gov

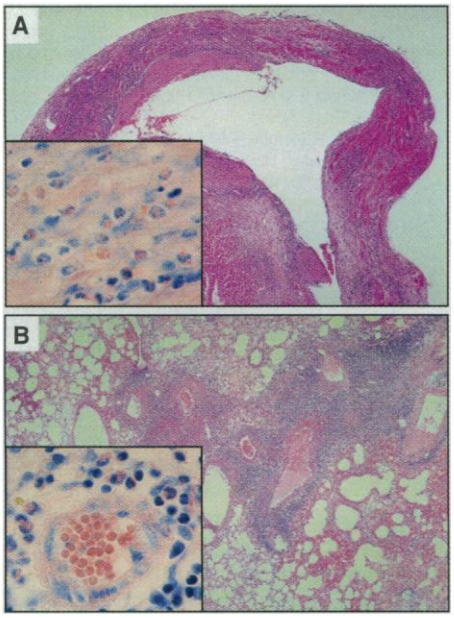

Fig. 2. Histology of heart and lungs from BCL-$6^{-/-}$ mice. (**A**) Myocarditis, low-power view, hematoxylin and eosin stain. Inset: high-power view, Giemsa stain. (**B**) Pulmonary vasculitis, low-power view, hematoxylin and eosin stain. Inset: high power-view, Giemsa stain.

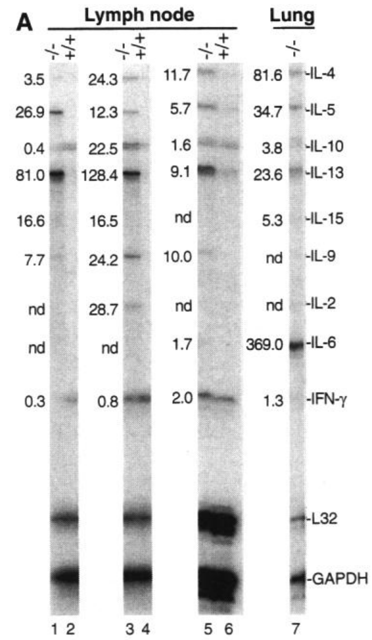

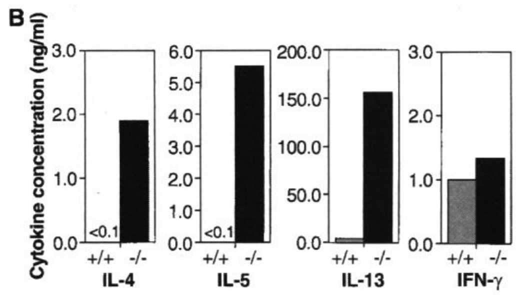

Fig. 4. Cytokine mRNA expression in BCL-$6^{-/-}$ mice. (**A**) RNase protection assay of multiple cytokine mRNAs induced by anti-CD3 activation of T cells from BCL-$6^{-/-}$ or wild type (+/+) mice. In vitro cultures were prepared with lymph node cells (lanes 1 through 4 and 6 through 7) or pulmonary inflammatory cells (lane 5). Pairs of BCL-$6^{-/-}$ and wild-type mice from the same litter were analyzed (litter 1, lanes 1 and 2; litter 2, lanes 3 and 4; litter 3, lanes 5 through 7). Assays are representative of results from BCL-$6^{-/-}$ lymph nodes (n = 6), wild-type lymph nodes (n = 7), and BCL-$6^{-/-}$ pulmonary inflammatory cells (n = 2). A Storm phosphoimager system (Molecular Dynamics) was used to quantitate the pixel intensity of each cytokine band, which was divided by the sum of the intensities in the control L32 and glyceraldehyde phosphate dehydrogenase (GAPDH) bands in the same lane for normalization. The ratio of cytokine expression in each BCL-$6^{-/-}$ mouse relative to its wild-type littermate control is shown at the left of each cytokine band. nd, not determined. (**B**) ELISA's of IL-4, IL-5, IL-13, and IFN-γ produced after anti-CD3 activation of T cells from BCL-$6^{-/-}$ or wild-type (+/+) mice. Cultures of inflammatory cells from hearts and lungs of BCL-$6^{-/-}$ mice (n = 3) were compared with a culture of hematopoietic cells pooled from the hearts and lungs of 10 wild-type control mice and tested. The average cytokine concentration in the three BCL-$6^{-/-}$ cultures is presented. <0.1 = cytokine concentration was below the sensitivity limit of the assay (0.1 ng/ml).

in these animals, some relatively healthy BCL-$6^{-/-}$ mice had histological evidence of myocarditis or pulmonary vasculitis or both. Inflammatory disease was not detected in the gut, kidneys, or skin of BCL-$6^{-/-}$ mice.

A second prominent phenotype of BCL-$6^{-/-}$ mice was revealed when we immunized the healthiest BCL-$6^{-/-}$ mice with the T cell–dependent antigen trinitrophenyl-conjugated keyhole limpet hemocyanin (TNP-KLH) (*13*). The germinal center immune response was evaluated by immunohistochemical staining (*13*) of spleen sections with peanut agglutinin (PNA) to identify germinal center B cells and antibodies to immunoglobulin D (IgD) to identify non–germinal center B cells (*14, 15*) (Fig. 3). Spleens from wild-type immunized mice (Fig. 3B) showed a large increase in the number of germinal centers as compared with unimmunized mice (Fig. 3A). Although the spleens of unimmunized BCL-$6^{-/-}$ mice had normal primary follicles (Fig. 3C), immunized BCL-$6^{-/-}$ mice did not develop germinal centers (Fig. 3D). Rather, the BCL-$6^{-/-}$ spleens were enlarged by a granulocytic infiltrate (Fig. 3D) consisting largely of eosinophils (*16*).

We measured the ability of the BCL-$6^{-/-}$ mice to make antibodies to TNP in response to TNP-KLH (*13*). The concentrations of primary IgM antibodies to TNP in BCL-$6^{-/-}$ mice and wild-type control mice were comparable, whereas BCL-$6^{-/-}$ mice were severely impaired in their ability to make secondary IgG antibodies to TNP of all subclasses (Fig. 3E). In contrast, immunization of BCL-$6^{-/-}$ mice with the T cell–independent antigen TNP-Ficoll elicited IgM and

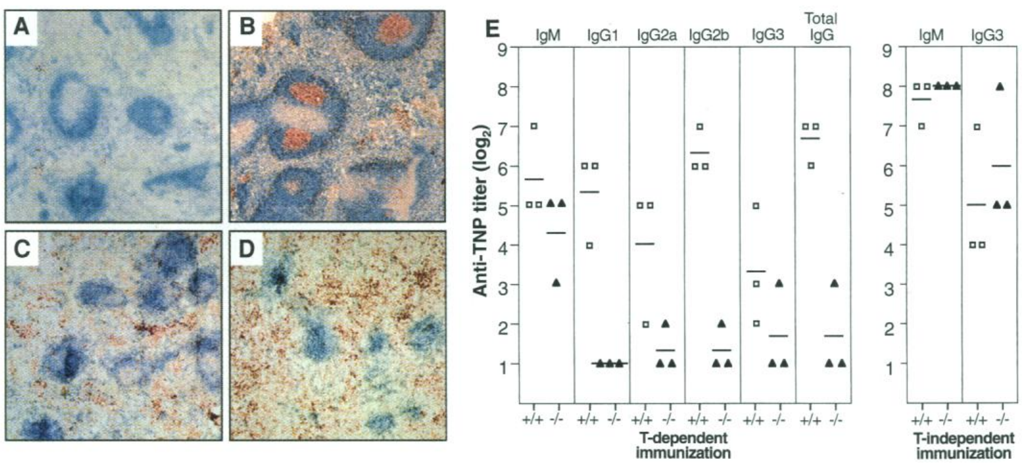

Fig. 3. Analysis of immune responses of BCL-$6^{-/-}$ mice. Spleen sections were stained with PNA (red) to reveal germinal center cells and with antibodies to IgD (blue) to reveal B cell follicles. The intensely staining brown cells in (C) and (D) are granulocytes that have high endogenous peroxidase activity. (**A**) Wild-type unimmunized littermate. (**B**) Wild-type littermate immunized with TNP-KLH. (**C**) Unimmunized BCL-$6^{-/-}$ mouse. (**D**) BCL-$6^{-/-}$ mouse immunized with TNP-KLH. (**E**) Titers of antibodies to TNP of various Ig subclasses after immunization with TNP-KLH (left panel) or TNP-Ficoll (right panel) (*13*). The $\log_2$ titers from three BCL-$6^{-/-}$ or wild-type mice are shown with a bar representing the mean. Unimmunized mice generally had anti-TNP titers of 1 $\log_2$.

IgG3 anti-TNP titers that were indistinguishable from those of wild-type mice (Fig. 3E). The selective defect of BCL-$6^{-/-}$ mice in generating an IgG antibody response to a T cell–dependent antigen is in keeping with the inability of these mice to mount a germinal center reaction.

To understand further the pathogenesis of the inflammatory disease in BCL-$6^{-/-}$ mice, we immunophenotyped the inflammatory cells from the lungs of mice with severe pulmonary vasculitis and detected monocytes/macrophages, granulocytes, and $CD4^+$ T lymphocytes (*16*). To test whether T cells from BCL-$6^{-/-}$ mice might abnormally express cytokines, we activated T cells in vitro with antibodies to the CD3 component of the T cell receptor and monitored the expression of cytokine mRNAs with a ribonuclease (RNase) protection assay (*17*) (Fig. 4A). BCL-$6^{-/-}$ lymph node cultures had elevated interleukin-4 (IL-4), IL-5, and IL-13 mRNA levels when compared to cultures from wild-type littermate controls. Notably, BCL-$6^{-/-}$ mice and their littermate controls expressed interferon-γ (IFN-γ) mRNA comparably (Fig. 4A), and IL-12 p40 mRNA was not detected in these cultures (*16*). Activation of T cells from pulmonary inflammatory lesions yielded elevated IL-4, IL-5, IL-6, and IL-13 mRNA, with low or no expression of IL-2, IL-9, IL-10, IL-15, and IFN-γ mRNAs (Fig. 4A, lane 7). Cytokine enzyme-linked immunosorbant assays (ELISAs) revealed increased production of IL-4, IL-5, and IL-13 in cultures of BCL-$6^{-/-}$ inflammatory cells without a comparable increase in IFN-γ production (Fig. 4B).

IL-4, IL-5, IL-6, and IL-13 are all cytokines that are produced primarily by the T helper cell type 2 (T_H2) subset of T lymphocytes, whereas IFN-γ is a hallmark of T_H1 cells (*18, 19*). Development of T_H2 cells is dependent on the Stat6 transcription factor, which is activated during IL-4 signaling (*20*). Signal transducers and activators of transcription (STAT) transcription factors recognize the GAS motif (*21*), which bears a previously unrecognized resemblance to the BCL-6 consensus DNA binding site (*6, 8, 22, 23*). Gel mobility-shift DNA binding assays (*24*) revealed that BCL-6 could bind well to an IL-4–responsive GAS motif in the CD23b promoter (*25*) that was also a binding site for Stat6 (*26*) (Fig. 5A). We next tested the ability of BCL-6 to repress transcription through the CD23b GAS element cloned upstream of the thymidine kinase promoter. In a transient transfection assay (*27*), BCL-6 modestly repressed basal transcription but blocked the Stat6-dependent activation of this reporter gene by IL-4 in a concentration-dependent manner (Fig. 5B).

Finally, we investigated whether BCL-6 could inhibit expression of the endogenous CD23 gene in a B cell line, WI-L2-NS, which up-regulates CD23 in response to IL-4 treatment (*24*). WI-L2-NS cells, which lack BCL-6 (*5*), were transiently transfected with expression vectors for BCL-6 and mouse ICAM, a cell surface protein that served as a marker for transfected cells (*28*). After transfection, IL-4 induced CD23 expression in the absence of BCL-6, but addition of BCL-6 decreased CD23 expression and blocked its IL-4 inducibility (Fig. 5C). These data suggest that CD23 may be a natural target gene for BCL-6 repression. Consistent with this notion, germinal center B cells, which express BCL-6 protein, do not express CD23 (*29*) even though other activated B cells do. More generally, these data show that BCL-6 may modify the outcome of IL-4 signaling in cells that express BCL-6.

The BCL-$6^{-/-}$ mouse revealed BCL-6 as a critical regulatory factor that determines the outcome of the immune response. In the absence of BCL-6, germinal centers and T cell–dependent antibody responses were not generated, whereas antibody responses to a T cell–independent antigen were normal. In contrast to some other mouse mutants that lack germinal centers (*30*), the architecture of secondary lymphoid organs in BCL-$6^{-/-}$ mice appeared histologically normal (Fig. 3C), and B and T cells proliferated normally in response to a variety of mitogenic stimuli in vitro (*31*) and had normal expression of several molecules that have been implicated in germinal center formation (*12*). Together with the selective expression of BCL-6 in all germinal center B cells and in a subset of

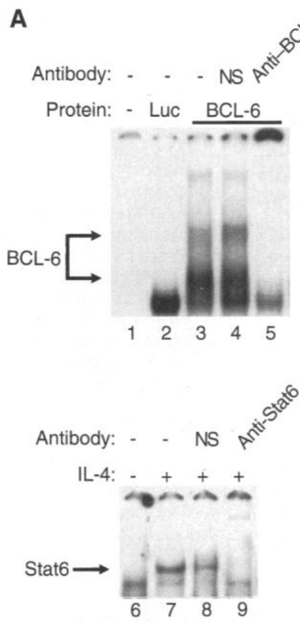

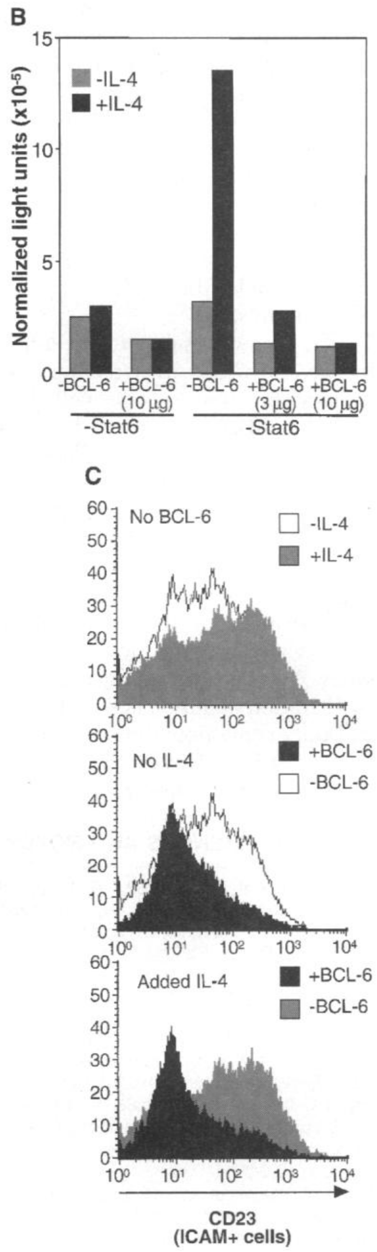

Fig. 5. Repression by BCL-6 of IL-4–induced expression of CD23. (**A**) Binding of BCL-6 and Stat6 to the IL-4–responsive element in the CD23b promoter. EMSA DNA binding assays were performed with the use of a radiolabeled CD23b binding site and in vitro–translated BCL-6 (lanes 3 through 5), luciferase (Luc) (lane 2), nuclear extracts from unstimulated WI-L2-NS cells (lane 6), or WI-L2-NS cells stimulated with IL-4 (lanes 7 through 9). Antibodies to BCL-6 (lane 5) or Stat6 (lane 9) or normal rabbit serum (NS) were included in the indicated reactions. (**B**) Repression by BCL-6 of an IL-4–responsive reporter construct. NIH 3T3 cells were transfected with a luciferase reporter construct containing a multimerized CD23b Stat6/BCL-6 site, and, in the indicated lanes, expression vectors for Stat 6 or BCL-6 or both. Transfected cells were either stimulated (black bars) or not stimulated (grey bars) with IL-4. Data are representative of three independent experiments. (**C**) Repression by BCL-6 of endogenous CD23 expression in a B cell line. WI-L2-NS cells were transfected with expression vectors for BCL-6 (or empty control vector) and the mouse ICAM cell surface protein as a marker of transfected cells. Transfected ICAM+ cells, treated or untreated with IL-4, were analyzed for cell surface expression of CD23 by flow cytometry. Data are representative of three independent experiments. Top panel: empty vector, no IL-4 (white histogram) versus empty vector, +IL-4 (grey histogram). Middle panel: BCL-6 expression vector, no IL-4 (black histogram) versus empty vector, no IL-4 (white histogram). Bottom panel: BCL-6 expression vector, +IL-4 (black histogram) versus empty vector, +IL-4 (grey histogram).

germinal center T cells (2–5), our findings define BCL-6 as an obligatory regulator of germinal center differentiation.

The BCL-$6^{-/-}$ mouse revealed a second and unanticipated function of BCL-6 in controlling inflammation. Our data suggest that abnormal production of T_H2-like lymphokines underlies the inflammation in BCL-$6^{-/-}$ mice. Consistent with this notion, the inflammatory heart and lung lesions showed pronounced eosinophilia that was likely due to local IL-5 production by T_H2 cells. Furthermore, after immunization with TNP-KLH, serum IgE levels were elevated in some BCL-$6^{-/-}$ mice, which is again a feature of T_H2 responses (19, 32). Because IL-4 signaling through Stat6 is required for the differentiation of naïve T cells into T_H2 cells (20, 33), BCL-6 could conceivably modulate this process by repressing Stat6-responsive genes. BCL-6 protein expression is high in germinal center T cells and in occasional T cells outside of the germinal center but is not detectable in resting or mitogenically activated T cells (2, 4), which suggests that BCL-6 might specifically block T_H2 differentiation during an antigen-driven immune response. Additionally, BCL-6 may regulate inflammation by modulating signaling by cytokines besides IL-4 because the BCL-6 DNA recognition motif resembles the binding sites for several STAT factors.

The present results provide a framework for investigations into the molecular pathology of diffuse large cell lymphoma caused by dysregulation of BCL-6 expression. The aberrant lymphokine regulation in BCL-$6^{-/-}$ mice and the potential of BCL-6 to repress transcription by binding to STAT sites raises the possibility that constitutive expression of BCL-6 in diffuse large cell lymphoma might influence the responsiveness of the lymphoma cells to extrinsically or intrinsically derived cytokines. A full understanding of the abnormal proliferation of diffuse large cell lymphomas will only come from detailed knowledge of the role of BCL-6 in cytokine signaling and in the germinal center reaction.

REFERENCES AND NOTES

1. B. H. Ye *et al.*, *Science* **262**, 747 (1993); A. Migliazza *et al.*, *Proc. Natl. Acad. Sci. U.S.A.* **92**, 12520 (1995); T. Miki, N. Kawamata, S. Hirosawa, N. Aoki, *Blood* **83**, 26 (1994); J. P. Kerckaert *et al.*, *Nature Genet.* **5**, 66 (1993); B. W. Baron *et al.*, *Proc. Natl. Acad. Sci. U.S.A.* **90**, 5262 (1993); F. LoCoco *et al.*, *Blood* **83**, 1757 (1994); T. Otsuki *et al.*, *ibid.* **85**, 2877 (1995); C. Bastard *et al.*, *ibid.* **83**, 2423 (1994).
2. T. Onizuka *et al.*, *Blood* **86**, 28 (1995).
3. L. Flenghi *et al.*, *Am. J. Pathol.* **147**, 405 (1995).
4. G. Cattoretti *et al.*, *Blood* **86**, 45 (1995).
5. D. Allman *et al.*, *ibid.* **87**, 5257 (1996).
6. V. L. Seyfert, D. Allman, Y. He, L. M. Staudt, *Oncogene* **12**, 2331 (1996).
7. P. Dhordain *et al.*, *ibid.* **11**, 2689 (1995); C. Deweindt *et al.*, *Cell Growth Differ.* **6**, 1495 (1995).
8. C.-C. Chang, B. H. Ye, R. S. K. Chaganti, R. Dalla-Favera, *Proc. Natl. Acad. Sci. U.S.A.* **93**, 6947 (1996).
9. B. H. Koller and O. Smithies, *ibid.* **86**, 8932 (1989).
10. Two BCL-6 genomic fragments derived from a strain 129/Sv genomic library (Stratagene) were cloned on either side of the PGK-neoR cassette in the vector pPNT (34): A 7.5-kb Eco RI fragment, containing much of the BCL-6 coding region and with the 3′ Eco RI site corresponding to the unique Eco RI site in the BCL-6 cDNA and with a 3.5-kb Spe-Xho fragment corresponding to 3′ noncoding region. Isolation of embryonic stem cells with a targeted BCL-6 locus and subsequent generation of BCL-$6^{-/-}$ mice with the use of these cells was performed with standard techniques (9). BCL-$6^{-/-}$ mice used in these experiments resulted from intercrosses between the 129 strain from which the ES cells were derived and strain C57B1/6.
11. Mice were immunized intraperitoneally with 100 μg of TNP-KLH in complete Freund's adjuvant (CFA). After 12 days, splenocytes were lysed and immunoprecipitated with the indicated antibodies. Immunoprecipitates were electrophoresed through a 7.5% SDS–polyacrylamide gel electrophoresis gel, transferred to nitrocellulose, incubated, and developed with a rabbit antibody to BCL-6 (5), with the use of the ECL system (Amersham).
12. Bone marrow cells, splenocytes, and thymocytes were analyzed by flow cytometry for the following surface proteins: CD4, CD8, CD45R (B220), IgM, CD3, CD24 (HSA), CD43, CD11b (Mac1), Gr-1, CD90 (Thy-1), CD5, IgD, TCR-αβ, CD25, CD23, CD38, CD80 (B7.1), CD86 (B7.2), MHC class II (IA), CD11a (LFA-1), CD19, CD18, CD40 ligand, CTLA-4, and CD-69. No differences between BCL-6 mutant mice and wild-type littermate control mice were observed.
13. Mice 5 to 6 weeks old were immunized intraperitoneally with 100 μg of TNP-KLH in CFA. After 12 days, serum was collected for anti-TNP titers, and spleens were processed for immunohistochemistry by being embedded in OCT compound (Tissue-Tek) and frozen. Splenic cryosections were stained with PNA-horseradish peroxidase, biotin–anti-mouse IgD, and streptavidin-alkaline phosphatase according to standard procedures (15). For T cell–independent immunization, mice were injected intraperitoneally with 25 μg of TNP-conjugated Ficoll suspended in phosphate-buffered saline. Serum was collected for anti-TNP titers after 7 days. Anti-TNP titers were assayed from sera by ELISA on TNP-ovalbumin–coated plates with the use of alkaline phosphatase–conjugated, goat anti-mouse Ig antibodies specific for various Ig isotypes (Southern Biotech).
14. I. C. M. MacLennan, *Annu. Rev. Immunol.* **12**, 117 (1994).
15. J. Jacob and G. Kelsoe, *J. Exp. Med.* **176**, 679 (1992).
16. A. Dent, unpublished observations.
17. Tissue culture dishes were coated with monoclonal antibody (mAb) (20 μg/ml) to CD3 (145-2C11, Pharmingen). For analysis of cytokine mRNA expression, 20 × 10^6 lymph node cells, or 7 × 10^6 lung inflammatory cells were cultured on the anti-CD3 coated plates at 5 × 10^6 per milliliter for 48 hours. Total cellular RNA from each sample was analyzed with a multiple cytokine RNase protection assay (Pharmingen) according to the manufacturer's specifications. For cytokine ELISA assays, cells were cultured at 2 × 10^6 per milliliter on anti-CD3 coated plates for 24 hours before collection of supernatants. ELISA antibodies and standards were obtained from Pharmingen (IFN-γ and IL-4), A. Sher (IL-5), and R&D Systems (IL-13). To prepare lung and heart inflammatory cells, tissues were minced, ground between glass slides, and filtered through a 70-μm nylon mesh.
18. T. R. Mosmann, H. Cherwinski, M. W. Bond, M. A. Giedlin, R. L. Coffman, *J. Immunol.* **136**, 2348 (1986).
19. R. A. Seder, *Annu. Rev. Immunol.* **12**, 635 (1994); A. K. Abbas, K. M. Murphy, A. Sher, *Nature* **383**, 787 (1996).
20. K. Takeda *et al.*, *Nature* **380**, 627 (1996); K. Shimoda *et al.*, *ibid.*, p. 630; M. H. Kaplan, U. Schindler, S. T. Smiley, M. J. Grusby, *Immunity* **4**, 313 (1996).
21. C. Schindler and J. E. J. Darnell, *Annu. Rev. Biochem.* **64**, 621 (1995).
22. N. Kawamata *et al.*, *Biochem. Biophys. Res. Commun.* **204**, 366 (1994); B. W. Baron *et al.*, *Genes Chromosomes Cancer* **13**, 221 (1995).
23. The BCL-6 consensus DNA binding motif is TTC(C/T)T(A/C)GAA. The STAT consensus DNA binding motif is TTCN_{3-4}GAA.
24. Electrophoretic mobility-shift assay (EMSA) DNA binding reactions were performed essentially as described (6). The CD23b DNA probe sequence is 5′-GATCAGGGTGAATTTCTAAGAAAGGGACTGGTGT-3′. BCL-6 protein and the luciferase control protein were generated with in vitro translation as described (6). Nuclear extracts were prepared essentially as described (35). For antibody supershift analysis, 3 μg of antibody [anti–BCL-6 (N3) or anti-Stat6 (S20); Santa Cruz Biotechnology] or preimmune rabbit serum was used.
25. I. Kohler and E. P. Rieber, *Eur. J. Immunol.* **23**, 3066 (1993).
26. J. Hou *et al.*, *Science* **265** (1994); H. Kotanides and N. C. Reich, *ibid.* **262**, 1265 (1993); C. Schindler, H. Kashleva, A. Pernis, R. Pine, P. Rothman, *EMBO J.* **13**, 1350 (1994).
27. A CD23b luciferase reporter construct was prepared by tandem ligation of three human CD23b BCL-6/Stat6 sites (24) immediately 5′ to a minimal TK promoter (base pairs −81 to +52) in pGL2basic (Promega). NIH 3T3 cells were transfected by the calcium phosphate transfection method using 2 μg of β-galactosidase (β-Gal) expression vector (pSV2Bgal), 5 μg of CD23b reporter plasmid, 10 μg of Stat6 expression plasmid (in the vector pCEV27) or empty pCEV27 vector, and 10 μg of BCL-6 expression vector [pCGN-BCL-6 (6)] or empty pCGN vector control. The day after transfection, cells were incubated for 16 hours in serum-free medium and then treated with 500 U/ml (0.25 ng/ml) of mouse IL-4 for 6 hours. Cell extracts were prepared and analyzed with the Luciferase Assay System (Promega). Luciferase activity was normalized on the basis of β-Gal activity in each extract.
28. 4 × 10^6 WI-L2-NS cells were transfected with 6 μg of marker expression vector for mouse intercellular adhesion molecule–1 (ICAM) (pmICAM) and 30 μg of expression vector for BCL-6 [pCGN BCL-6 (6)] or empty vector (pCGN) using a BTX electroporator set at 260 V, 950 mF, and 720 ohms. After overnight culture, the transfected cells were stimulated with recombinant human IL-4 (10 ng/ml; Genzyme) for 16 hours and subsequently stained for flow cytometry with mouse anti-human CD23-PE (M-L233, Pharmingen) and hamster anti-mouse CD54/ICAM (3E2, Pharmingen).
29. V. Pascual *et al.*, *J. Exp. Med.* **180**, 329 (1994).
30. M. Matsumoto *et al.*, *Science* **271**, 1289 (1996); M. Pasparakis, L. Alexopoulou, V. Episkopou, G. Kollias, *J. Exp. Med.* **184**, 1397 (1996).
31. B cells were stimulated by lipopolysaccharide (LPS), LPS + IL-4, antibodies to IgM, or CD40 ligand. T cells were stimulated by concanavalin A, phorbol 12-myristate 13-acetate + ionomycin, or antibodies to CD3. The proliferative responses of BCL-$6^{-/-}$ and wild-type lymphocytes were comparable.
32. BCL-$6^{-/-}$ mice (n = 5) had, on average, 3.1 μg/ml of serum IgE after immunization with TNP-KLH in CFA, whereas wild-type littermates (n = 6) had 0.36 μg/ml of serum IgE.
33. M. Kopf *et al.*, *Nature* **362**, 245 (1993).
34. V. L. Tybulewicz, C. E. Crawford, P. K. Jackson, R. T. Bronson, R. C. Mulligan, *Cell* **65**, 1153 (1991).
35. E. Schrieber, P. Mattias, M. M. Muller, W. Schaffner, *Nucleic Acids Res.* **17**, 6419 (1989).

36. We thank B. Koller for valuable assistance in the generation of BCL-$6^{-/-}$ mice and for helpful discussions; G. Miller, M. Raffeld, D. Levens, S. Mackem, and A. Cheever for help with pathological examination of BCL-$6^{-/-}$ mice; J. Inman for TNP-Ficoll; W. LaRochelle for the Stat6 expression vector; P. Caspar and A. Sher for help with the anti–IL-5 ELISA and helpful discussions; B. Paul for recombinant mouse IL-4 and helpful discussions; K. Kelly for the pmICAM expression plasmid; and T. Waldmann, R. Germain, R. Hodes, and H. Morse for helpful discussions. Mice were maintained according to the NIH Office of Animal Care and Use guidelines.

6 February 1997; accepted 25 March 1997